



## Colloidally stable surface-modified iron oxide nanoparticles: Preparation, characterization and anti-tumor activity



Hana Macková<sup>a</sup>, Daniel Horák<sup>a,\*</sup>, Georgiy Viktorovich Donchenko<sup>b</sup>,  
Vadim Ivanovich Andriyaka<sup>b</sup>, Olga Mikhailovna Palyvoda<sup>b</sup>,  
Vladimir Ivanovich Chernishov<sup>b</sup>, Vasyl Fedorovich Chekhun<sup>c</sup>, Igor Nikolaevich Todor<sup>c</sup>,  
Oleksandr Ivanovich Kuzmenko<sup>b</sup>

<sup>a</sup> Institute of Macromolecular Chemistry, AS CR, Heyrovsky Sq. 2, 162 06 Prague 6, Czech Republic

<sup>b</sup> Palladin Institute of Biochemistry, NASU, 9 Leontovich St., 01601 Kiev, Ukraine

<sup>c</sup> R. E. Kavetsky Institute of Experimental Pathology, Oncology and Radiobiology, NASU, 45 Vasylykivska St., 03022 Kiev, Ukraine

### ARTICLE INFO

#### Article history:

Received 30 June 2014

Received in revised form

16 September 2014

Accepted 16 September 2014

Available online 18 September 2014

#### Keywords:

Iron oxide nanoparticle

Poly(*N,N*-dimethylacrylamide-*co*-acrylic acid)

Protein oxidation

Oxidative stress

Antimetastatic activity

### ABSTRACT

Maghemite ( $\gamma$ -Fe<sub>2</sub>O<sub>3</sub>) nanoparticles were obtained by co-precipitation of Fe(II) and Fe(III) chlorides and subsequent oxidation with sodium hypochlorite and coated with poly(*N,N*-dimethylacrylamide-*co*-acrylic acid) [P(DMAAm-AA)]. They were characterized by a range of methods including transmission electron microscopy (TEM), elemental analysis, dynamic light scattering (DLS) and zeta potential measurements. The effect of superparamagnetic P(DMAAm-AA)- $\gamma$ -Fe<sub>2</sub>O<sub>3</sub> nanoparticles on oxidation of blood lipids, glutathione and proteins in blood serum was detected using 2-thiobarbituric acid and the ThioGlo fluorophore. Finally, mice received magnetic nanoparticles administered *per os* and the antitumor activity of the particles was tested on Lewis lung carcinoma (LLC) in male mice line C57BL/6 as an experimental *in vivo* metastatic tumor model; the tumor size was measured and the number of metastases in lungs was determined. Surface-modified  $\gamma$ -Fe<sub>2</sub>O<sub>3</sub> nanoparticles showed higher antitumor and antimetastatic activities than commercial CuFe<sub>2</sub>O<sub>4</sub> particles and the conventional antitumor agent cisplatin.

© 2014 Elsevier B.V. All rights reserved.

## 1. Introduction

Iron oxide nanoparticles show many potential biomedical applications, for instance, in targeted drug delivery and controlled drug release [1], especially in preclinical and clinical oncology as contrast agents for magnetic resonance imaging (MRI) [2], in specific cell labeling and separation, hyperthermia [3], or biocatalysis [4]. Both magnetite (Fe<sub>3</sub>O<sub>4</sub>) and maghemite ( $\gamma$ -Fe<sub>2</sub>O<sub>3</sub>) nanoparticles are often used in these applications. They have to fulfill a range of requirements including a spherical shape, appropriate diameter with a narrow particle size distribution, high saturation magnetization, the presence of functional groups suitable for attachment of target biomolecules and minimal non-specific adsorption [5].

Magnetic iron oxide nanoparticles can be prepared by a number of methods, *e.g.*, alkaline co-precipitation of iron salts [6], thermal decomposition of organometallic precursors [7–11] or hydrothermal process [12]. Since the surface of superparamagnetic nanoparticles plays a key role in their prospective specific

application, many reports focus on different modifications of iron oxides [13–17]. Recently, several reports described nanoparticles capable of inducing production of reactive oxygen species (ROS) leading to oxidative stress and cytotoxicity [18]. Examples of such particles include titanium dioxide, carbon black, polystyrene and cobalt-chromium alloy [19]. Cytotoxic response of cancer cells to iron oxide nanoparticles was also investigated [13].

We are reporting here a simple preparation of water-dispersible magnetic iron oxide nanoparticles coated with poly[*N,N*-dimethylacrylamide-*co*-(acrylic acid)] P(DMAAm-AA) which is suitable for subsequent modification of the particles. Preliminary model biological experiments are also described envisaging application of such particles in cancer treatment.

## 2. Methods

### 2.1. Materials

FeCl<sub>2</sub> · 4H<sub>2</sub>O, FeCl<sub>3</sub> · 6H<sub>2</sub>O, *N,N*-dimethylacrylamide (DMAAm), 2,2'-azobisisobutyronitrile (AIBN), NaCl, Tris, thiobarbituric acid,

\* Corresponding author.

E-mail address: [horak@imc.cas.cz](mailto:horak@imc.cas.cz) (D. Horák).

trichloroacetic acid and copper iron oxide ( $\text{CuFe}_2\text{O}_4$ ), cell cultivation medium 199 and *cis*-diaminoplatinum(II) dichloride (cisplatin) were obtained from Sigma-Aldrich (St. Louis, MO, USA). Sodium hypochlorite solution was from Bochemie (Bohumín, Czech Republic). Fluorescent ThioGlo thiol reagent was from Calbiochem (San Diego, CA, USA). Acrylic acid (AA) was from Hexion Specialty Chemicals (Sokolov, Czech Republic), other reagents and solvents were from LachNer (Neratovice, Czech Republic). Ultrapure Q water ultrafiltered in a Milli-Q Gradient A10 system (Millipore, Molsheim, France) was used for the preparation of solutions.

## 2.2. Preparation of $\gamma\text{-Fe}_2\text{O}_3$ nanoparticles modified with poly(*N,N*-dimethylacrylamide-co-acrylic acid) [DMAAm- $\gamma\text{-Fe}_2\text{O}_3$ ]

$\gamma\text{-Fe}_2\text{O}_3$  nanoparticles were prepared by alkaline co-precipitation of  $\text{FeCl}_2$  and  $\text{FeCl}_3$  (1:2 mole ratio) in aqueous  $\text{NH}_3$  solution according to a method described earlier [6]. *N,N*-Dimethylacrylamide (3 g) and acrylic acid (0.33 g) were dissolved in a mixture of toluene (3.5 ml) and THF (3.4 ml) and AIBN initiator (10 mg) was added. Polymerization was performed at 70 °C for 8 h under magnetic stirring. The resulting P(DMAAm-AA) copolymer was precipitated into heptane and dried in vacuum (0.13 Pa). Finally, a solution of P(DMAAm-AA) (5 mg) in water (1 ml) was added to a  $\gamma\text{-Fe}_2\text{O}_3$  colloid (1 ml; 50 mg  $\gamma\text{-Fe}_2\text{O}_3$ /ml).

## 2.3. Blood serum preparation

Blood (~4 ml) was taken by heart puncture with a polyethylene syringe from intact 250–300 g Wistar rat immediately after euthanasia and transferred into a glass centrifuge tube. The tube was left standing at room temperature for 30 min. The clotted blood was then centrifuged for 15 min at 1500 g. The blood serum was collected from the supernatant and stored at –80 °C in polystyrene tubes.

## 2.4. Blood lipid oxidation

Blood serum (25  $\mu\text{l}$  in 0.9% NaCl and 10 mM Tris, pH 7.4) containing certain amounts of nanoparticles was incubated at 37 °C for 24 h under shaking. Neat blood serum served as a control. Lipid oxidation was monitored by measuring of thiobarbituric acid reactive substances (TBARS), which are formed as a byproduct by the reaction of thiobarbituric acid and compounds resulting from the decomposition of polyunsaturated fatty acid lipid peroxides [20]. After incubation, a mixture of 0.375% thiobarbituric acid, 15% trichloroacetic acid and 0.25 M HCl was added to blood serum or malondialdehyde standards at 1:2 (v/v) ratio. The mixtures were incubated at 95 °C for 30 min and protein pellets were separated by centrifugation at 3000 g for 15 min. An aliquot was monitored at 540 nm using a MQX 200 BioTek spectrophotometer (Winooski, VT, USA).

## 2.5. Glutathione and blood protein oxidation

To determine the effect of nanoparticles on the oxidation of a non-enzymatic antioxidant glutathione and of blood protein, protein-oxidation markers were investigated *in vitro* in the presence or presence of nanoparticles using a commercial thiol-specific fluorophore ThioGlo [21, 22]. The incubation mixture contained blood serum (25  $\mu\text{l}$ /ml),  $\gamma\text{-Fe}_2\text{O}_3$  or P(DMAAm-AA)- $\gamma\text{-Fe}_2\text{O}_3$  or  $\text{CuFe}_2\text{O}_4$  nanoparticles (10, 25 and 100 mg/l) in 0.9% NaCl solution and 10 mM Tris (pH 7.4). The mixtures were incubated at 37 °C for 24 h under shaking. In order to determine the activity of glutathione, aliquots of the nanoparticle suspensions were incubated in blood serum at 37 °C for 24 h under

shaking (20 rpm) and the ThioGlo fluorophore was added to reach 10  $\mu\text{M}$  concentration. To analyze blood protein oxidation, an aliquot of the nanoparticle suspension was treated with ThioGlo fluorophore in 2% sodium dodecyl sulfate solution for 30 min. Fluorescence was detected using a FLX 800 BioTek spectrofluorimeter at excitation and emission wavelengths 388 and 500 nm, respectively.

## 2.6. Anti-tumor and anti-metastatic activity of P(DMAAm-AA)- $\gamma\text{-Fe}_2\text{O}_3$ nanoparticles

Lewis lung carcinoma (LLC; a metastatic tumor model) in male mice C57BL/6, body weight of 23 g, was used as an experimental *in vivo* model. 0.2 ml of LLC cells ( $2 \times 10^6$  cells per animal) were injected into femoral muscle in cell culture medium 199. Experimental animals were divided into three groups. First group did not receive any medication (except saline) and served as a tumor control. The second group received 1.2 mg of administered cisplatin per kg intraperitoneally, typically on day 11 after LLC transplantation, when the tumor size reached 2–3 mm. The third group received P(DMAAm-AA)- $\gamma\text{-Fe}_2\text{O}_3$  nanoparticles (30 mg/kg) *per os* into the stomach. In the second and third groups, the animals received six injections during 28 days. At the end of the experiment, the tumor size was measured and the number of metastases in lungs was calculated.

## 2.7. Ethical issues of animals use

All experiments involving small laboratory animals of non-transgenic strain, such as male mice (C57BL/6 strain), were performed according to the EC regulations on animal experimentation and after approval of the ethical committees of Palladin Institute of Biochemistry and R. E. Kavetsky Institute of Experimental Pathology, Oncology and Radiobiology. The animals were housed in a specialized animal facility under appropriate conditions. Euthanasia of animals was performed by necropsy after asphyxiation with carbon dioxide.

## 2.8. Physicochemical and biological characterization

Morphology of the nanoparticles was investigated using a Tecnai Spirit G2 transmission electron microscope (TEM; FEI; Brno, Czech Republic). Number-average diameters ( $D_n$ ), weight-average diameters ( $D_w$ ) and polydispersity indexes  $\text{PDI} = D_w/D_n$  were calculated using Atlas software (TESCAN Digital Microscopy Imaging, Brno, Czech Republic) by counting at least 500 particles on TEM microphotographs. The  $D_n$  and  $D_w$  can be expressed as follows:  $D_n = \sum D_i/N$ ;  $D_w = \sum D_i^4/\sum D_i^3$ , where  $N$  is the number of particles. The hydrodynamic diameters  $D_h$ , polydispersities PI and zeta potentials were determined by dynamic light scattering (DLS) with an Autosizer Lo-C (Malvern Instruments; Malvern, UK). Elemental analyses were performed on a Perkin-Elmer 2400 CHN apparatus (Norwalk, CT, USA). Size exclusion chromatography (SEC) measurements were performed on a gradient Knauer system (Berlin, Germany) using diode array detection (DAD) and Alltech 3300 evaporative light scattering detection (ELSD). The measurements were performed on a Phenomenex PolySept-GFC-P linear column using an isocratic system of 0.03 M ammonium acetate buffer in  $\text{CH}_3\text{CN}/\text{water}$  (20:80).

Blood lipid oxidation analysis was made using a MQX 200 BioTek spectrophotometer (Winooski, VT, USA). Glutathione and blood protein oxidation assays were performed using a FLX 800 BioTek spectrofluorimeter.

Magnetic properties were measured using a SQUID MPMS5 magnetometer (Quantum Design, San Diego, CA, USA) at 300 K.

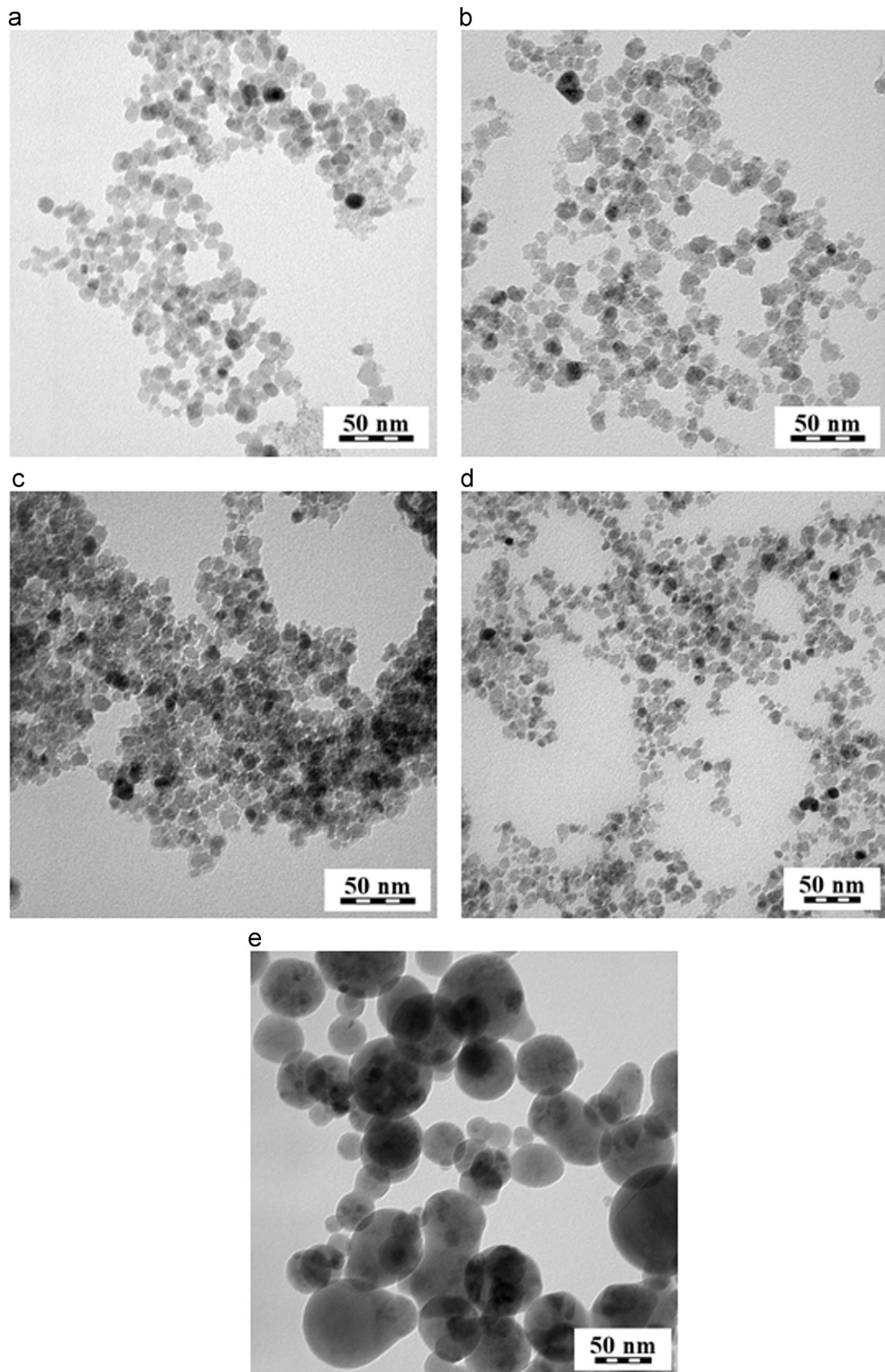


**Fig. 1.** TEM micrographs of neat  $\gamma\text{-Fe}_2\text{O}_3$  (a, c) and P(DMAAm-AA)- $\gamma\text{-Fe}_2\text{O}_3$  nanoparticles (b, d) immediately after the synthesis (a, b) and after three-year storage at 4 °C (c, d).  $\text{CuFe}_2\text{O}_4$  (e).

### 3. Results and discussion

P(DMAAm-AA) copolymer was obtained by the AIBN-initiated polymerization of the respective monomers in a toluene/THF solution. The P(DMAAm-AA) copolymer contained 55.3 and 9.2 wt% of C and N, respectively (the calculated values were 59.5 and 12.7 wt%). We can speculate that the soluble P(DMAAm-AA) with a low content of AA was removed by washing. The copolymer had  $M_w=50,400$  Da with moderate polydispersity (PDI=1.4). Hence, the copolymer was considered a promising and efficient stabilizer of particle dispersions in aqueous media. Moreover, acrylic acid (AA) was included in the copolymer to facilitate its attachment to the iron oxide surface via carboxyl groups which are known to complex with iron ions [6, 23–25].

The morphology, size and polydispersity of both neat  $\gamma\text{-Fe}_2\text{O}_3$  and P(DMAAm-AA)- $\gamma\text{-Fe}_2\text{O}_3$  nanoparticles were monitored by TEM (Fig. 1). Both types of the nanoparticles are of similar size (9 nm) with PDI = 1.3–1.4 indicating a satisfactorily narrow particle size distribution. Even though the polymer coating was not visible in TEM, the P(DMAAm-AA)- $\gamma\text{-Fe}_2\text{O}_3$  nanoparticles were more separated (Fig. 1b) than the uncoated  $\gamma\text{-Fe}_2\text{O}_3$  particles, the latter were overlapping (Fig. 1a). Obviously, P(DMAAm-AA) coating did not allow contacts of particles thus hindering their aggregation. TEM micrographs of the nanoparticles after three-year storage at 4 °C are shown in Fig. 1c and d. The figures thus confirmed that the modification of  $\gamma\text{-Fe}_2\text{O}_3$  nanoparticle surface with P(DMAAm-AA) was highly efficient preventing the nanoparticle aggregation even after a long time. Compared with the neat  $\gamma\text{-Fe}_2\text{O}_3$  (54 nm), hydrodynamic size of the P(DMAAm-AA)- $\gamma\text{-Fe}_2\text{O}_3$  particles according to DLS increased to 86 nm (Fig. 2) and polydispersity PI became almost unchanged (0.14–0.19). Polydispersity (DLS) was thus in agreement with the polydispersity index (TEM). The large discrepancy in the size values obtained by TEM and DLS consists in the fact that the former method measures the number-average diameters of the particles in the dry state, whereas the latter provides the z-average of the particles in water. Zeta potential and pH of  $\gamma\text{-Fe}_2\text{O}_3$  and P(DMAAm-AA)- $\gamma\text{-Fe}_2\text{O}_3$  particles decreased from  $-48.8$  to  $-42.5$  mV and from 10.1 to 5.9, respectively, due to presence of COOH groups in the P(DMAAm-AA) copolymer shell.

Magnetic character of the synthesized nanoparticles was analyzed by a magnetometer (Fig. 3). Saturation and remanent magnetization and coercivity of the neat  $\gamma\text{-Fe}_2\text{O}_3$  were 53 and  $1.37 \text{ A m}^2 \text{ kg}^{-1}$  and  $1.69 \text{ kA m}^{-1}$ , respectively. In contrast, saturation magnetization of the coated nanoparticles was  $33 \text{ A m}^2 \text{ kg}^{-1}$  and coercivity and remanent magnetization was the same as in the neat  $\gamma\text{-Fe}_2\text{O}_3$ . The lower saturation magnetization of the neat

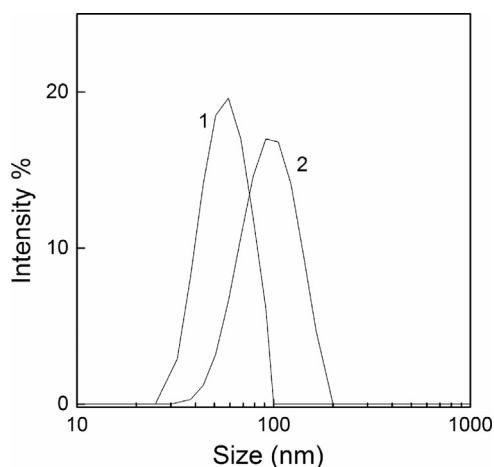


Fig. 2. DLS of  $\gamma\text{-Fe}_2\text{O}_3$  (1) and P(DMAAm-AA)- $\gamma\text{-Fe}_2\text{O}_3$  (2) nanoparticles.

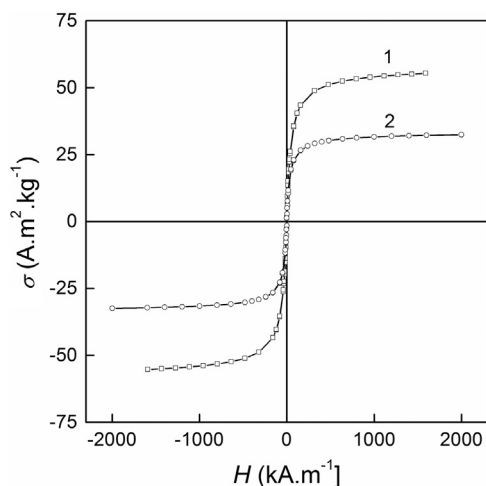


Fig. 3. Hysteresis loops of  $\gamma\text{-Fe}_2\text{O}_3$  (1) and P(DMAAm-AA)- $\gamma\text{-Fe}_2\text{O}_3$  (2) nanoparticles at 300 K.

nanoparticles than that of the bulk state ( $60\text{--}80 \text{ A m}^2 \text{ kg}^{-1}$ ) [26] indicates the presence of impurities or some amorphous materials and could be also caused by long storage before the measurement [27]. Magnetic properties of the neat  $\gamma\text{-Fe}_2\text{O}_3$  particles were described in a more detail elsewhere [28].

Peroxidation of blood serum lipids, oxidation of glutathione and protein oxidation initiated with 40 nm  $\text{CuFe}_2\text{O}_4$  (Fig. 1e),  $\gamma\text{-Fe}_2\text{O}_3$  and P(DMAAm-AA)- $\gamma\text{-Fe}_2\text{O}_3$  (at 4.4–444  $\mu\text{g/ml}$ ) were investigated *in vitro* (Fig. 4). All the studied  $\text{CuFe}_2\text{O}_4$  and  $\gamma\text{-Fe}_2\text{O}_3$  nanoparticles at a concentration of 444  $\mu\text{g/ml}$  statistically significantly increased the blood serum lipid peroxidation (Fig. 4a). Surprisingly, the highest concentration of released TBARS was induced by copper ferrite, and this strong peroxidation effect was not detected by other used methods. The lipid peroxidation in the presence of P(DMAAm-AA)- $\gamma\text{-Fe}_2\text{O}_3$  nanoparticles at the above concentration was almost the same as that in the presence of unmodified nanoparticles (Fig. 4a). PDMAAm coating thus did not deteriorate interaction of lipids with the iron oxide, but prevented the aggregation and increased the available reactive surface. As expected, the lipid peroxidation increased with increasing concentration of particles in the medium.

Oxidation of both glutathione and proteins in blood serum with  $\text{CuFe}_2\text{O}_4$ , neat and coated  $\gamma\text{-Fe}_2\text{O}_3$  nanoparticles was observed at the concentration 444  $\mu\text{g/ml}$  (Fig. 4b and c). P(DMAAm-AA)- $\gamma\text{-Fe}_2\text{O}_3$  nanoparticles oxidized glutathione and proteins more efficiently than the neat  $\gamma\text{-Fe}_2\text{O}_3$  particles or copper ferrite. The enhanced oxidation can be explained by smaller size of coated  $\gamma\text{-Fe}_2\text{O}_3$  than of  $\text{CuFe}_2\text{O}_4$  nanoparticles. Moreover, P(DMAAm-AA)- $\gamma\text{-Fe}_2\text{O}_3$  colloid was distinguished by absence of aggregates which could substantially decrease the specific surface area available for interactions with glutathione and/or proteins.

Finally, the animals with Lewis lung carcinoma treated with P(DMAAm-AA)- $\gamma\text{-Fe}_2\text{O}_3$  nanoparticles as well as healthy animals and those with untreated tumors were investigated *in vivo* (Fig. 5). The treatment of animal tumors with the above nanoparticles decreased the tumor size. Moreover, anti-tumor as well as anti-metastatic activities of the P(DMAAm-AA)- $\gamma\text{-Fe}_2\text{O}_3$  particles in the animal Lewis lung carcinoma model were examined (Fig. 6a and b). The effects were compared with those of  $\text{CuFe}_2\text{O}_4$  and cisplatin. P(DMAAm-AA)- $\gamma\text{-Fe}_2\text{O}_3$  nanoparticles at a concentration of 30 mg/kg significantly suppressed both tumor growth and metastasis formation. An equal or even better cytostatic effect of P(DMAAm-AA)- $\gamma\text{-Fe}_2\text{O}_3$  nanoparticles was observed compared with cisplatin. We can thus suppose that higher amounts of lipid radicals and other reactive oxygen species were produced under Fe

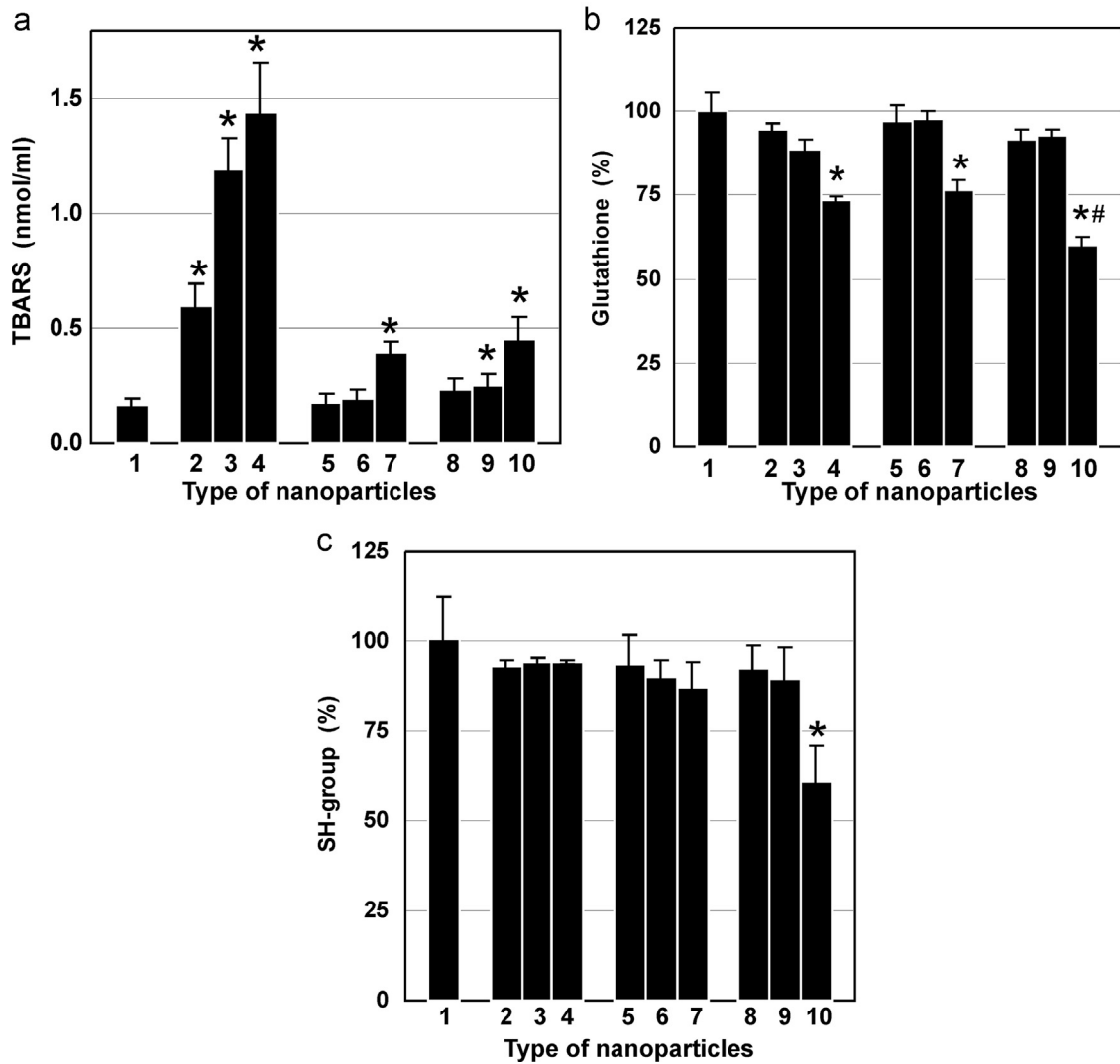


**Fig. 4.** *In vitro* oxidation of (a) lipids, (b) glutathione and (c) protein thiols in blood serum in the presence of nanoparticles 1–10. Blood serum (25 µl/ml) was incubated at 37 °C for 24 h in the absence of nanoparticles (1) or in the presence of CuFe<sub>2</sub>O<sub>4</sub> (2–4), γ-Fe<sub>2</sub>O<sub>3</sub> (5–7) and P(DMAAm-AA)-γ-Fe<sub>2</sub>O<sub>3</sub> (8–10) nanoparticles: 4.4 µg of particles/ml (2, 5, 8), 44 µg/ml (3, 6, 9) and 444 µg/ml (4, 7, 10). The data are mean ± SE (n=5–8). \*Statistically significant difference compared with oxidation in the absence of nanoparticles (1). #Statistically significant difference compared with CuFe<sub>2</sub>O<sub>4</sub> (4) and γ-Fe<sub>2</sub>O<sub>3</sub> nanoparticles (7). TBARS – thiobarbituric acid reactive substances.

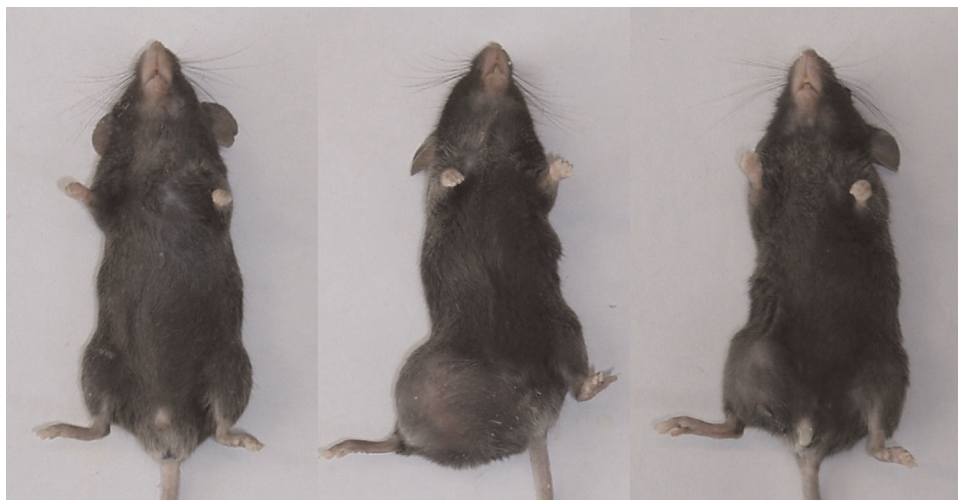


**Fig. 5.** Antitumor effect of P(DMAAm-AA)-γ-Fe<sub>2</sub>O<sub>3</sub> nanoparticles on Lewis lung carcinoma model in C57BL/6 mice. From left to right: control, untreated mouse with a tumor and mouse with a tumor treated with P(DMAAm-AA)-γ-Fe<sub>2</sub>O<sub>3</sub> nanoparticles *per os*.

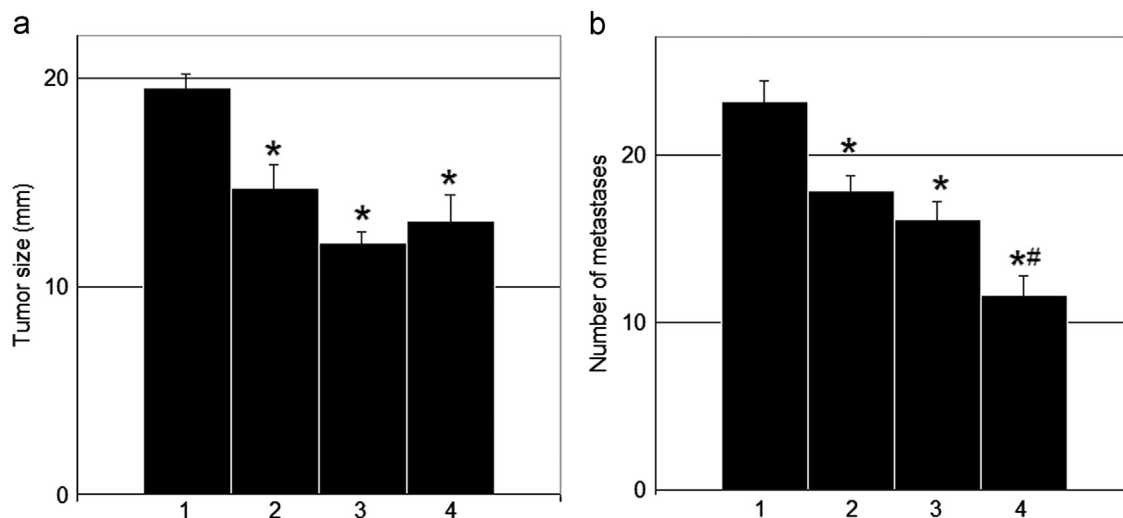


**Fig. 6.** Antitumor (a) and antimetastatic (b) activity of nanoparticles in *in vivo* animal Lewis lung carcinoma model. No treatment (1), 1.2 mg cisplatin (2), 30 mg CuFe<sub>2</sub>O<sub>4</sub> (3) and 30 mg P(DMAAm-AA)- $\gamma$ -Fe<sub>2</sub>O<sub>3</sub> nanoparticles per kg of body weight (4). The data are mean  $\pm$  SE ( $n=5-8$ ). \*Statistically significant difference from control animals. #Statistically significant difference from CuFe<sub>2</sub>O<sub>4</sub> nanoparticles (3).

(II) catalysis compared with the healthy cells. Although some of the radicals could be eliminated by the antioxidant protective system of the cells, the remaining radicals oxidatively damaged lipids, proteins and glutathione in membranes and intracellular proteins. This mechanism thus explains a decrease in the size of animal tumors treated with P(DMAAm-AA)- $\gamma$ -Fe<sub>2</sub>O<sub>3</sub> nanoparticles.

#### 4. Conclusions

In the present report, alkaline co-precipitation in water of FeCl<sub>2</sub> and FeCl<sub>3</sub> followed by oxidation with NaOCl produced *ca.* 10 nm superparamagnetic maghemite nanoparticles with a narrow particle size distribution. A P(DMAAm-AA) copolymer was synthesized, serving as a coating of magnetic nanoparticles, to provide their colloidal stability by complexation of carboxyl groups of the copolymer with the iron oxide surface. The P(DMAAm-AA)- $\gamma$ -Fe<sub>2</sub>O<sub>3</sub> nanoparticle colloids were stable even three years after their synthesis.

In biological experiments, the effects of the iron oxide and copper ferrite nanoparticles on oxidation of blood lipids, glutathione and proteins were investigated. Experiments with oxidation of lipids in blood serum demonstrated that both neat  $\gamma$ -Fe<sub>2</sub>O<sub>3</sub> and P(DMAAm-AA)- $\gamma$ -Fe<sub>2</sub>O<sub>3</sub> nanoparticles (444  $\mu$ g/ml) induced an extensive lipid peroxidation, which was approximately three times higher in the presence of the particles than in their absence. Very high lipid oxidation was then observed with CuFe<sub>2</sub>O<sub>4</sub> nanoparticles. The results of blood lipid oxidation with  $\gamma$ -Fe<sub>2</sub>O<sub>3</sub> and P(DMAAm-AA)- $\gamma$ -Fe<sub>2</sub>O<sub>3</sub> were in agreement with those obtained in a study of consumption of the glutathione thiol group. Compared with experiments in the absence of the nanoparticles, both neat  $\gamma$ -Fe<sub>2</sub>O<sub>3</sub> (also CuFe<sub>2</sub>O<sub>4</sub>) and P(DMAAm-AA)- $\gamma$ -Fe<sub>2</sub>O<sub>3</sub> nanoparticles decreased the concentration of thiol groups by 25% and 40%, respectively. Finally, oxidation of proteins in the presence of neat  $\gamma$ -Fe<sub>2</sub>O<sub>3</sub>, CuFe<sub>2</sub>O<sub>4</sub> and P(DMAAm-AA)- $\gamma$ -Fe<sub>2</sub>O<sub>3</sub> nanoparticles was studied. Whereas the neat  $\gamma$ -Fe<sub>2</sub>O<sub>3</sub> and CuFe<sub>2</sub>O<sub>4</sub> particles did not oxidize the proteins, those of P(DMAAm-AA)- $\gamma$ -Fe<sub>2</sub>O<sub>3</sub> increased the oxidation by 40% compared with the experiments in the absence of the particles.

After completion of the *in vitro* experiments, the P(DMAAm-AA)- $\gamma$ -Fe<sub>2</sub>O<sub>3</sub> nanoparticles were tested *in vivo* on Lewis lung carcinoma (LLC) in male mice line C57BL/6. The efficiency of the treatment was compared with that of cisplatin and CuFe<sub>2</sub>O<sub>4</sub> nanoparticles as control. While CuFe<sub>2</sub>O<sub>4</sub> was an example of commercially

available highly magnetic nanoparticles with a pronounced redox activity, cisplatin was used as a standard anticancer drug for comparison. The developed P(DMAAm-AA)- $\gamma$ -Fe<sub>2</sub>O<sub>3</sub> nanoparticles showed higher antitumor and antimetastatic activities than both CuFe<sub>2</sub>O<sub>4</sub> and cisplatin probably due to an enhanced oxidative stress in tumor cells. To conclude, P(DMAAm-AA)- $\gamma$ -Fe<sub>2</sub>O<sub>3</sub> nanoparticles provide a promising tool in cancer therapy.

#### Acknowledgment

Financial support of European Commission (DiaTools Project no. 259796) and Ministry of Education, Youth and Sports of the Czech Republic (Project LH14318) is gratefully acknowledged. This work was supported also by grant from BIOCEV – Biotechnology and Biomedicine Centre of Academy of Sciences and Charles University in Vestec, project supported from European Regional Development Fund (Project CZ.1.05/1.1.00/02.0109). The authors wish to acknowledge the Academy of Sciences of the Czech Republic and the National Academy of Sciences of Ukraine for their support of the joint research project.

#### References

- [1] M.M. Yallapu, S.F. Othman, E.T. Curtis, N.A. Bauer, N. Chauhan, D. Kumar, M. Maggi, S.C. Chauhan, *Int. J. Nanomed.* 7 (2012) 1761.
- [2] M.M. Yallapu, S.F. Othman, E.T. Curtis, B.K. Gupta, M. Jaggi, S.C. Chauhan, *Biomaterials* 32 (2011) 1890.
- [3] A.P. Khandhar, R.M. Ferguson, J.A. Simon, K.M. Krishnan, *J. Biomed. Mater. Res. A* 100 (2012) 728.
- [4] Y. Kang, L. Zhou, X. Li, J. Yuan, *J. Mater. Chem.* 21 (2011) 3704.
- [5] L.A. Harris, J.D. Goff, A.Y. Carmichael, J.S. Riffle, J.J. Harburn, T.G. Pierre St., M. Saunders, *Chem. Mater.* 15 (2003) 1367.
- [6] M. Babič, D. Horák, P. Jendelová, K. Glogarová, V. Herynek, M. Trchová, K. Likavčanová, P. Lesný, E. Pollert, M. Hájek, E. Syková, *Bioconjug. Chem.* 20 (2009) 283.
- [7] W.W. Yu, J.C. Falkner, C.T. Yavuz, V.L. Colvin, *Chem. Commun.* 20 (2004) 2306.
- [8] K. Simeonidis, S. Mourdikoudis, M. Moulla, I. Tsiaoussis, C. Martinez-Boubeta, M. Angelakeris, C. Dendrinos-Samara, O. Kalogirou, *J. Magn. Magn. Mater.* 316 (2007) e1.
- [9] S. Sun, H. Zeng, *J. Am. Chem. Soc.* 124 (2002) 8204.
- [10] S. Sun, H. Zeng, D.B. Robinson, S. Raoux, P.M. Rice, S.X. Wang, G. Li, *J. Am. Chem. Soc.* 126 (2004) 273.
- [11] J. Park, K. An, Y. Hwang, J.-G. Park, H.-J. Noh, J.-Y. Kim, J.-H. Park, N.-M. Hwang, T. Hyeon, *Nat. Mater.* 3 (2004) 891.
- [12] X. Sun, C. Zheng, F. Zhang, Y. Yang, G. Wu, A. Yu, N. Guan, *J. Phys. Chem. C* 113 (2009) 16002.

- [13] A. Petri-Fink, B. Steitz, A. Finka, J. Salaklang, H. Hofmann, *Eur. J. Pharm. Biopharm.* 68 (2008) 129.
- [14] H.K. Patra, N.U. Khaliq, T. Romu, E. Wiechec, M. Borga, A.P.F. Turner, A. Tiwari, *Adv. Healthc. Mater.* 3 (2013) 526.
- [15] X. Li, H. Li, W. Yi, J. Chen, B. Liang, *Int. J. Nanomed.* 8 (2013) 3019.
- [16] J. Zhou, J. Zhang, A.E. David, V.C. Yang, *Nanotechnology* 24 (2013) 375102.
- [17] A.A. McBride, D.N. Price, L.R. Lamoureux, A.A. Elmaoued, J.M. Vargas, N. L. Adolphi, P. Muttill, *Mol. Pharm.* 10 (2013) 3574.
- [18] G. Huang, H. Chen, Y. Dong, X. Luo, H. Yu, Z. Moore, E.A. Bey, D.A. Boothman, J. Gao, *Theranostics* 3 (2013) 116.
- [19] I. Papageorgiou, C. Brown, R. Schins, S. Singh, R. Newson, S. Davis, J. Fisher, E. Ingham, C.P. Case, *Biomaterials* 28 (2007) 2946.
- [20] D. Gelvan, P. Saltman, *Biochim. Biophys. Acta* 1035 (1990) 353.
- [21] M.E. Langmuir, J.-R. Yang, K.A. Le Compte, R.E. Durand, New thiol reactive fluorophores for intracellular thiols and glutathione measurement, *Fluorescence Microscopy and Fluorescent Probes*, Plenum Press, New York (1996) 229.
- [22] S.K. Wright, R.E. Viola, *Anal. Biochem.* 265 (1998) 8.
- [23] A.-H. Lu, E.L. Salabas, F. Schüth, *Angew. Chem. Int. Ed.* 46 (2007) 1222.
- [24] J. Rubio-Retama, N.E. Zafeiropoulos, C. Serafinelli, R. Rojas-Reyna, B. Voit, E. L. Cabarcos, M. Stamm, *Langmuir* 23 (2007) 10280.
- [25] M. Safi, J. Courtois, M. Seigneuret, H. Conjeaud, J.-F. Berret, *Biomaterials* 32 (2011) 9353.
- [26] R.M. Cornell, U. Schwertmann, *The Iron Oxides: Structure, Properties, Reactions, Occurrence and Uses*, VCH, New York (1996) 123.
- [27] E. Strable, J.W.M. Bulte, B. Moskowit, K. Vivekanandan, M. Allen, T. Douglas, *Chem. Mater.* 13 (2001) 2201.
- [28] A. Tocchio, D. Horák, M. Babič, M. Trchová, M. Veverka, M.J. Beneš, M. Šlouf, A. Fojtík, *J. Polym. Sci. A: Polym. Chem.* 47 (2009) 4982.